Preprints of the 21st IFAC World Congress (Virtual)
Berlin, Germany, July 12-17, 2020

Glocal Traction Control for In-wheel-motor Electric Vehicles - A Passivity Approach -

Binh-Minh Nguyen*, Koji Tsumura*, Shinji Hara**

**The University of Tokyo, **Tokyo Institute of Technology, Japan*

Abstract: Although traction control of in-wheel-motor electric vehicles (IWM-EVs) has been studied for years, we still face the essential theoretical issue: How to assure the stability of the overall system while attaining both global and local control performances? This issue has been neglected by almost the works in the literature. The main reason is due to the nonlinearity and complexity in vehicle dynamics, especially the vehicle driven by multi-actuators. A new traction method is proposed in this paper in the glocal (global/local) framework to overcome this problem. The command to each local IWM includes two signals: (i) the local signal through anti-slip control in the lower-layer, and (ii) the global signal distributed from the driver or the upper-layer controller that managing the average wheel velocity. Stability of the whole system is guaranteed based on the fundamental passivity theory. The effectiveness of the proposed approach is verified by using Carsim/Matlab co-simulator.

Keywords: in-wheel-motor, electric vehicle, multi-agent system, traction control, passivity.

1. INTRODUCTION

Motion control of electric vehicles (EVs) has been an interesting topic for nearly two decades, thanks to the remarkable merits of in-wheel-motor (IWM) actuators (Hori, 2004). Various motion control methods have been proposed, such as side slip angle control (Nguyen *et al*, 2013) and range extension control (Fujimoto *et al*, 2015). This paper focuses on the most basic issue of EV motion control. It is traction control which prevents loss traction of driven road wheels. As shown in Table 1, traction control of EV includes four main groups, namely (I) wheel slip ratio control, (II) anti-slip control, (III) wheel velocity control, and (IV) wheel driving force control.

The number of IWM actuators has increased, from the two-IWM-COMS designed by Toyota to the eight-IWM-KAZ at Keio University (Shimizu, 2001). With the development of IWM technology (Sato *et al*, 2016), EVs driven by more than ten IWMs will be soon realized. This uptrend makes EV more powerful, flexible, and safer. An approach to utilize the benefit efficiently is to consider this kind of IWM-EV as a special type of multi-agent system (Nguyen *et al*, 2016a, 2017, 2019) as illustrated in Fig. 1. Each wheel is a local agent that physically interacts with each other to generate the global motion of the vehicle body as well as its local motion. Almost the previous researches that neglected the physical interaction face a non-trivial issue. That is how to theoretically guarantee the stability of the overall system by taking the nonlinearity of tire force characteristics properly.

The basic idea of this paper comes from the concept of "***glocal (global/local) control***," in which the control actions are restricted locally while the purposes are to achieve both the local and global behaviours (Hara *et al*, 2015). This concept has been applied in EV motion control by different

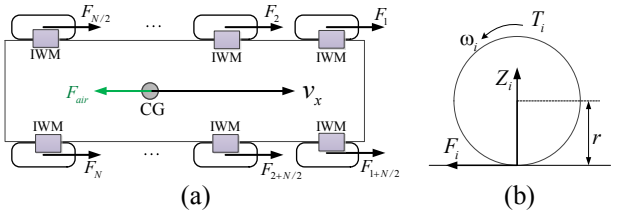

Fig. 1. IWM-EV as a multi-agent system [8]:
(a) Vehicle body, (b) Local motion of single wheel.

aspects as follows: We clarified the necessity of analysing the EV system as a whole based on "generalized frequency variable representation" (Nguyen *et al*, 2016b). A hierarchically decentralized motion control system was established based on "shared model set" (Nguyen *et al*, 2017). Recently, we presented a new hierarchical LQR strategy for optimal control of driving force (Nguyen *et al*, 2019a). However, the linearization of the vehicle dynamics is required for "generalized frequency variable" and "shared model set" approaches; and time-varying modelling is essential for our hierarchical LQR algorithm.

This paper contributes a more convenient design method for IWM-EV traction control based on passivity theory. The term passivity-based-control (PBC) was introduced thirty years ago as an approach to the adaptive control problem of rigid robots (Ortega *et al*, 1989). PBC has been attracted by control society worldwide, thanks to its convenience in system stabilization. In recent years, PBC has been applied in large scale dynamical control systems such as robot networks (Hatanaka *et al*, 2015) and electric power networks (Tsumura *et al*, 2018). This paper firstly shows that IWM-EV can be modelled as a hierarchically interconnected system. The lower-layer is composed of the local wheel dynamics, and the upper-layer is the vehicle body dynamics. The local wheels interact with each other through the aggregation and

Table 1. Review of traction control methods for electric vehicles

Group	Objective	Scheme	Comments	References
(I)	Wheel slip ratio control	Nonlinear control (sliding-mode)	- Chattering problem - Physical interaction is neglected	Amodeo *et al*, 2010
		Linear control by linearizing the tire slip dynamics	- Linearization is complex - Physical interaction is neglected	Hori *et al*, 1998
		Linear control by hierarchical LQR	- Time-varying model is required - *Physical interaction is considered*	Nguyen *et al*, 2019a
(II)	Anti-slip control	Zero-slip-model following control	- Optimal traction is not assured - Physical interaction is neglected	Li *et al*, 2006
		Maximum transmissible torque estimation	- Optimal traction is not assured - Physical interaction is neglected	Yin *et al*, 2009
		Based on wheel velocity control	- The system is simple to implement - The physical interaction is neglected	Suzuki *et al*, 2010
(III)	Wheel velocity control	Driving torque distribution by local wheel velocity control	- Simple linearized model is required - *Physical interaction is considered*	Nguyen *et al*, 2016b
		Hierarchically decentralized control of vehicle and wheel velocity	- Simple linearized model is required - *Physical interaction is considered*	Nguyen *et al*, 2017
(IV)	Wheel driving force control	Direct driving force control based on PI controller	- Driving force dynamics is poorly modelled - Physical interaction is neglected	Amada *et al*, 2012
		Driving force control based on wheel velocity and virtual variable control	- Control configuration is complex - Physical interaction is neglected	Maeda *et al*, 2013
		Linear control by hierarchical LQR	-Time-varying model is required - *Physical interaction is considered*	Nguyen *et al*, 2016a

distribution channels that connect two layers. Two traction control strategies, namely Strategies 1 and 2, are established utilizing this model. For the both strategies, a local controller $C_{l,i}$ is designed at each wheel. The output of $C_{l,i}$ is the local control signal $T_{l,i}$ for preventing the slip even if road condition varies. In Strategy 1, the actual IWM torque is the sum of $T_{l,i}$ and $T_{r,i}$ which is distributed from the driver's driving command T_{cmd}. Unlike Strategy 1, the signal $T_{r,i}$ in Strategy 2 is distributed from a signal T_g which is the output of a upper-layer controller C_g that manages the average wheel velocities. The stability of Strategies 1 and 2 can be guaranteed by applying the passivity theory to the feedback systems. Note that stability of the overall system can be maintained even if a single wheel is disconnected from the traction control system. Moreover, by suitably distributing the torque from T_{cmd} or T_g to $T_{r,i}$, additional control objectives can be attained. The traction control in this paper can be classified into group II in Table 1. The original idea was presented at IEEE VPPC 2019 (Nguyen *et al*, 2019b), in which the motion control system is completely decentralized and the linear tire force model is used for passivity analysis. This paper extends the PBC idea to the hierarchically decentralized control system, and the passivity is analysed using nonlinear tire force model.

2. MODEL OF IWM-EV

We consider an EV driven by N IWMs as shown in Fig. 1 (N is an even number). Let m be the total mass of the vehicle, J be the wheel inertia, and r be the wheel radius. T_i is the torque generated by IWM. The longitudinal force (driving force) and the vertical force at each wheel are denoted by F_i and Z_i, respectively. F_{air} represents the air resistance. The longitudinal velocity of the vehicle is v_x while ω_i is the rotational velocity of the wheel. Let $\mathbf{1}_N$ be the all-one-column-vector of size N, and define the following vectors:

$$\mathbf{T} = \begin{bmatrix} T_1 & \dots & T_N \end{bmatrix}^{\mathrm{T}},\ \mathbf{F} = \begin{bmatrix} F_1 & \dots & F_N \end{bmatrix}^{\mathrm{T}}, \boldsymbol{\omega} = \begin{bmatrix} \omega_1 & \dots & \omega_N \end{bmatrix}^{\mathrm{T}}$$

The motion of the vehicle body ($\boldsymbol{\mathcal{V}}$) is given by

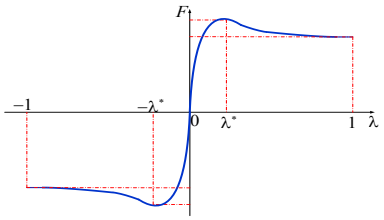

Fig. 2. Typical example of tire force characteristics.

$$m\dot{v}_x = \mathbf{1}_N^{\mathrm{T}}\mathbf{F} - F_{air} \tag{1}$$

Neglecting the wind velocity, the air resistance is given by

$$F_{air} = \rho v_x |v_x| \tag{2}$$

where ρ is the air resistance coefficient. On the other hand, the local motion of the wheel $\boldsymbol{\mathcal{W}}_i$ is

$$J\dot{\omega}_i = T_i - rF_i \tag{3}$$

Let ε be a small number to avoid division-by-zero, the slip ratio of the wheel is defined as

$$\lambda_i = \frac{r\omega_i - v_x}{\max\{r\omega_i, v_x, \varepsilon\}} \tag{4}$$

Fig. 2 describes the typical relationship between the driving force and the slip ratio (Jazar, 2008). The driving force gradually increases as the slip ratio increases from 0 to an optimal value λ^*. Since the slip ratio exceeds λ^*, the driving force is decreased to a minimum value as the slip ratio approaches to 1. The tire force is usually modelled by an empirical function, namely "magic formula" (Pacejka, 2012):

$$F_i(\lambda_i) = \begin{cases} f_i(\lambda_i) & \text{if } \lambda_i \geq 0 \\ -f_i(-\lambda_i) & \text{if } \lambda_i < 0 \end{cases} \tag{5}$$

$$\text{with } f_i(\lambda_i) = A_i \sin\left\{B_i \tan^{-1}\left[C_i\lambda_i - D_i\left(C_i\lambda_i - \tan^{-1}\left(C_i\lambda_i\right)\right)\right]\right\}$$

where $A_i = \mu_i Z_i$ with the friction coefficient μ_i. The friction coefficient and the shape factors B_i, C_i and D_i are identified

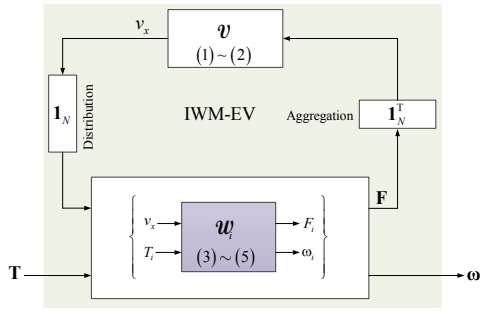

Fig. 3. Hierarchically decentralized model of IWM-EV.

from experiments. For instance, a typical set of parameters for the ice surface is $\{\mu_i, B_i, C_i, D_i\} = \{0.1, 2, 4, 1\}$.

Remark 1: The inequality $\lambda_i f_i(\lambda_i) \geq 0$ holds for any value of slip ratio λ_i in (-1, 1).

From (1) ~ (5), we can model the IWM-EV as a nonlinear multi-agent system with hierarchical structure as in Fig. 3.

3. PASSIVITY APPROACH TO IWM-EV

3.1 Fundamental of passivity theory

Consider a general system given by a state space equation

$$\begin{cases} \dot{x} = f(x,u) \\ y = h(x,u) \end{cases} \tag{6}$$

with input vector $u(t) \in \mathbb{R}^p$, output vector $y \in \mathbb{R}^p$, and the state vector $x(t) \in \mathbb{R}^n$. The input is assumed to be piecewise continuous in t and to be bounded for all $t \in \mathbb{R}_+$.

Definition 2 (Khalil, 2002): The system (6) from input u to output y is said to be passive if there exists a positive semidefinite function S: $\mathbb{R}^n \rightarrow \mathbb{R}_+$, called *storage function*, such that $\dot{S} = \frac{\partial S}{\partial x}\dot{x} \leq y^{\mathrm{T}}u$ holds for all $x \in \mathbb{R}^n$ and $u \in \mathbb{R}^p$. In addition, (6) is input strictly passive if $\dot{S} \leq y^{\mathrm{T}}u - \delta_u \|u\|^2$ for some $\delta_u > 0$, and output strictly passive if $\dot{S} \leq y^{\mathrm{T}}u - \delta_y \|y\|^2$ for some $\delta_y > 0$.

Considering the interconnected system in Fig. 4, the fundamental passivity theorems are stated as follows.

Theorem 3-a: The feedback connection system shown in Fig. 4 is passive with the input (ξ_1, ξ_2) and the output (y_1, y_2), if H_1 and H_2 are passive.

Theorem 3-b: If both subsystems H_1 and H_2 in Fig. 4 are output strictly passive, then the closed loop system H with input (ξ_1, ξ_2) and output (y_1, y_2) has a finite L_2-gain. Moreover, when $\xi_2 = 0$, the closed loop system with input ξ_1 and output y_1 has a finite L_2-gain if either (i) H_1 is passive and H_2 is input strictly passive, or (ii) H_1 is output strictly passive and H_2 is passive.

3.2 Passivity analysis of IWM-EV dynamics

Utilizing the **Definition 2** with the notice to **Remark 1**, we have the following proposition. The proof is similar to that of Propositions 1, 2, and 3 in the author's recent works (Nguyen *et al*, 2019b), so is omitted.

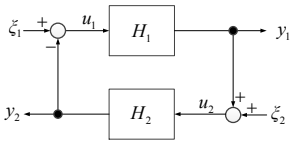

Fig. 4. Standard feedback connection of two subsystems.

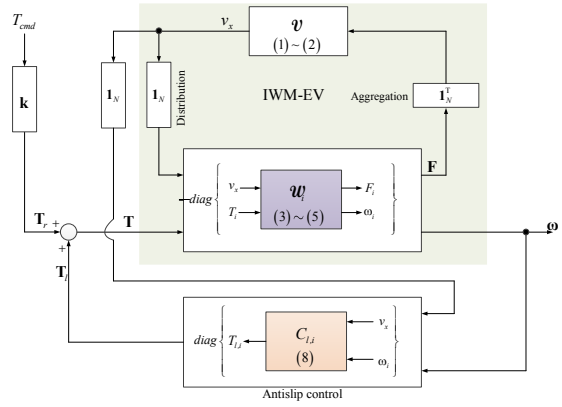

Fig. 5. Strategy 1: Decentralized traction control.

Proposition 4: The IWM-EV system is passive with the input $\mathbf{u} = \mathbf{T}$, the output $\mathbf{y} = \boldsymbol{\omega}$, and the storage function given as $S = S_{\mathrm{V}} + \sum_{i=1}^{N} S_{\mathrm{W},i}$ where $S_{\mathrm{V}} = \frac{1}{2}mv_x^2$ and $S_{\mathrm{W},i} = \frac{1}{2}J_i\omega_i^2$.

4. PASSIVITY BASED GLOCAL TRACTION CONTROL

Based on **Proposition 4**, we can simply design a motion control system for the IWM-EV, although it is a complex nonlinear system. For instance, we might design a strictly passive controller for feedback control of wheel velocities (Nguyen *et al*, 2019b). This paper will extend the PBC from wheel velocity control to anti-slip control, with the assumption that the vehicle velocity or its appropriate estimates are available.

4.1 Strategy 1-Decentralized traction control

This sub-section provides Strategy 1 for designing local controllers $C_{l,i}$ to guarantee the stability of total system. This control scheme is applicable when the torque command $\mathbf{T}_r = \begin{bmatrix} T_{r,1} & \dots & T_{r,N} \end{bmatrix}^{\mathrm{T}}$ is distributed to each wheel based on the driver's acceleration command T_{cmd}, i.e:

$$T_{r,i} = k_i \times T_{cmd} \tag{7}$$

where the ratio k_i satisfies $k_1 + \dots k_N = 1$ and $k_i > 0$. The distribution vector is $\mathbf{k} = \begin{bmatrix} k_1 & \dots & k_N \end{bmatrix}^T$. The system is described in Fig. 5, in which a possible option of the local control law $C_{l,i}$ for anti-slip control is given by

$$T_{l,i} = -K_{a,i}\left(r\omega_i - v_x\right) sign\left(\omega_i\right) sign\left(r\omega_i - v_x\right) - K_{\omega,i}\omega_i \tag{8}$$

where $K_{a,i}$ and $K_{\omega,i}$ are the control gains.

Proposition 5: The anti-slip control system in Fig. 5 with the local controller $C_{l,i}$ given by (8) is output strictly passive from the input $\mathbf{T}_r$ to the output $\boldsymbol{\omega}$ if the control gains are selected such that $K_{a,i} > 0$ and $K_{\omega,i} > 0$.

Proof: Select the storage function $S = S_{\mathrm{V}} + \sum_{i=1}^{N} S_{\mathrm{W},i}$. Then, it is readily seen from (1) ~ (3) that the derivative is given by

$$\dot{S} = m v_x \dot{v}_x + \sum_{i=1}^{N} J_i \omega_i \dot{\omega}_i = \left(\left(\sum_{i=1}^{N} F_i \right) - \rho v_x |v_x| \right) v_x + \sum_{i=1}^{N} J_i \omega_i \dot{\omega}_i \quad (9)$$

Note from Fig. 4 that we have

$$\boldsymbol{\omega}^{\mathrm{T}} \mathbf{T}_r = \boldsymbol{\omega}^{\mathrm{T}} \left(\mathbf{T} - \mathbf{T}_l \right) = \sum_{i=1}^{N} \omega_i \left(T_i - T_{l,i} \right) \quad (10)$$

This together with (3) ~ (5) and (9) leads to

$$\begin{aligned} \boldsymbol{\omega}^{\mathrm{T}} \mathbf{T}_r - \dot{S} &= \sum_{i=1}^{N} \left(\max\left\{ r\omega_i, v_x, \varepsilon \right\} \lambda_i f_i(\lambda_i) \right) + \left(\rho |v_x| \right) v_x^2 \\ &+ \sum_{i=1}^{N} K_{a,i} \left((r\omega_i - v_x) sign(r\omega_i - v_x) \right) \left(\omega_i sign(\omega_i) \right) + \sum_{i=1}^{N} K_{\omega,i} \omega_i^2 \end{aligned} \quad (11)$$

There exist four terms on the right-hand side of (11). It is clear from **Remark 1** that the first and second terms are always non-negative. Let define δ_ω be $\min\{K_{\omega,i}\} > 0$, then we can see that $\boldsymbol{\omega}^{\mathrm{T}} \mathbf{T}_r - \dot{S} \geq \sum_{i=1}^{N} K_{\omega,i} \omega_i^2 \geq \delta_\omega \left(\boldsymbol{\omega}^{\mathrm{T}} \boldsymbol{\omega} \right)$ holds. In other words,

$$\dot{S} \leq \boldsymbol{\omega}^{\mathrm{T}} \mathbf{T}_r - \delta_\omega \left(\boldsymbol{\omega}^{\mathrm{T}} \boldsymbol{\omega} \right) \quad (12)$$

holds true, which implies that the system is strictly passive.

4.3 Strategy 2- Hierarchical traction control

Next, we consider the situation such that $\mathbf{T}_r$ is not distributed from the driver, but from the upper motion control layer, i.e., in the autonomous driving system. Thanks to the anti-slip control law in the lower-layer given by (8), the average of the wheel's longitudinal velocity is quite closed to the vehicle velocity. Define the average rotational velocity of the wheels

$$\bar{\omega} = \left(\mathbf{1}_N^{\mathrm{T}} \boldsymbol{\omega} \right) / N \quad (13)$$

then, it is possible to control $r\bar{\omega}$ in the upper-layer, and distribute the global control signal to the lower-layer suitably. The Strategy 2 is described in Fig. 6, where $r\bar{\omega}^*$ can be treated as the reference of longitudinal velocity of the vehicle. The distribution vector **k** is defined similarly to the previous sub-section. Now, it is essential to investigate the lower-layer in Fig. 6. It is the system inside the red rectangular, with the input T_g and the output $r\bar{\omega}$.

Proposition 6: The lower-layer system (inside the dashed rectangular with red color) in Fig. 6 consisting of $\boldsymbol{\mathcal{W}}_i$, $C_{l,i}$ (i = 1,…, N) and $\boldsymbol{\mathcal{V}}$ is output strictly passive from the input T_g to the output $r\bar{\omega}$. Hence, the system depicted in Fig. 6 is stable if C_g is output strictly passive.

Proof: Let $\mathbf{T}_r = \begin{bmatrix} T_{r,1} & \dots & T_{r,N} \end{bmatrix}^{\mathrm{T}}$, we have $T_g = T_{r,1}/k_1 = \dots = T_{r,N}/k_N$, and: $r\bar{\omega}T_g = \frac{r}{Nk_1} T_{r,1}\omega_1 + \dots + \frac{r}{Nk_N} T_{r,N}\omega_N$. Since $0 < k_i < 1$, it is clear that $(1/k_i) > 1$. Consequently, the following inequality holds true

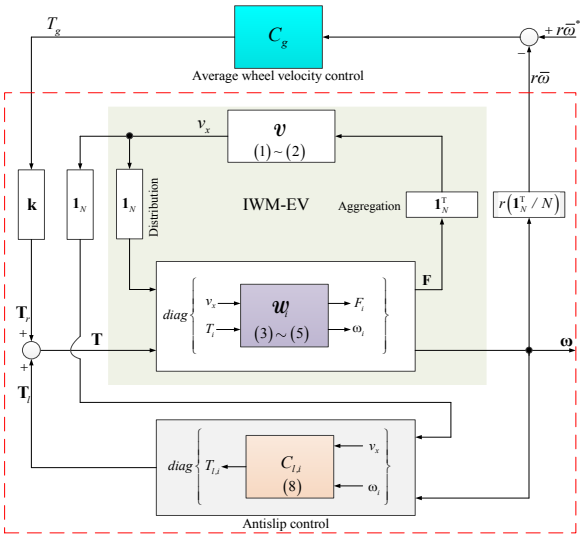

Fig. 6. Strategy 2: Hierarchical traction control.

$$r\bar{\omega}T_g > \frac{r}{N} \left(T_{r,1}\omega_1 + \dots + T_{r,N}\omega_N \right) = \frac{r}{N} \boldsymbol{\omega}^{\mathrm{T}} \mathbf{T}_r \quad (14)$$

As a result of **Proposition 5**, the lower-layer system in Fig. 6 is output strictly passive with the storage function

$$S = \frac{r}{N} \left(S_{\mathrm{V}} + \sum_{i=1}^{N} S_{\mathrm{W},i} \right) \quad (15)$$

Following the **Theorem 3**, if C_g is an output strictly passive transfer function, the stability of the overall system in Fig. 6 is assured. This completes the proof.

5. VERIFICATION BY SIMULATIONS

5.1 Simulation model

This paper utilizes Carsim/Matlab co-simulator to evaluate the proposed control methods. We selected the pickup vehicle model from the library of Carsim, although it is originally a gasoline vehicle model. To use this model for our purpose, it has been modified to be EV by establishing the IWM block in Matlab/Simulink, and the output torques of IWM are exported to Carsim through the ports IMP_MYUSM_*. The notation * represents the actuator index. By this way, we finally establish an electric pickup vehicle driven by four IWMs (N = 4). The vehicle mass without load is m_o = 1998 kg, and the maximum load capacity is 2000 kg. Each wheel's inertia and radius are J = 3.2 kgm^2 and r = 0.402 m, respectively.

5.2 Test1: Strategy 1 with energy management

Firstly, we evaluate the decentralized control system in Fig. 5. The driving command $\mathbf{T}_r$ is a vector of size 4. It is distributed from the total driving command T_{cmd} of the driver model:

$$T_{r,i} = k_i \times T_{cmd}, \quad i \in [1;4] \quad (16)$$

The distribution ratios updated in real-time in order to minimize the total output of the motors (Fujimoto *et al*, 2015). The driver accelerates the vehicle from the high friction surface (μ = 0.85) to the low friction surface (μ = 0.2) at t = 3.5 [s]. Notice that T_{cmd} is the same for two cases as follows:

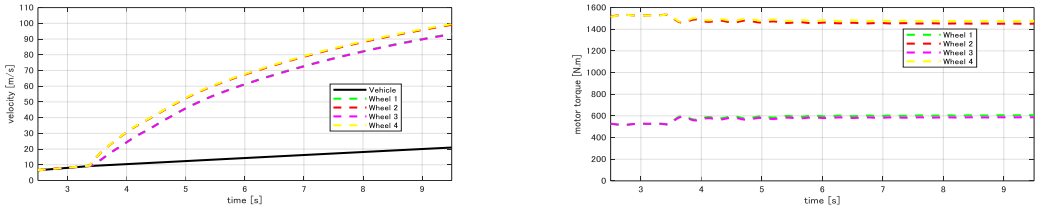

(a) Velocities. (b) Motor torques.

Fig. 7. **Test 1-a**: Without traction control.

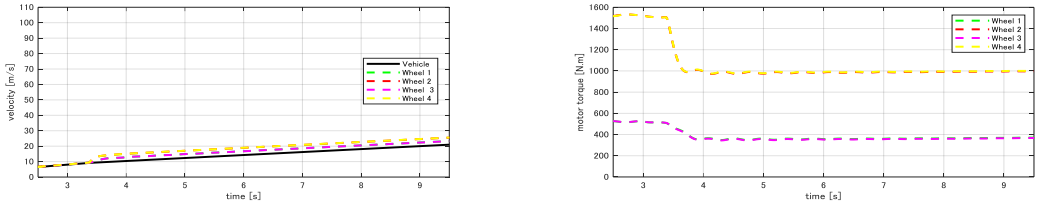

(a) Velocities. (b) Motor torques.

Fig. 8. **Test 1-b**: With traction control (Strategy 1).

Test 1-a (**Without traction control**): The control gains are set to be zero ($K_{a,i}$ = $K_{\omega,i}$ = 0). As seen in Fig. 7, all wheel velocities increase considerably in comparison with the vehicle velocity.

Test 1-b (**With traction control**): We utilize the control system in Fig. 5 in which the local controllers are designed as (8), which means that the acceleration is degraded if we increase $K_{\omega,i}$. On the other hand, the anti-slip performance would be worsen if $K_{a,i}$ is set smaller. By trial-and-error, a pair of local control gains is chosen as {$K_{a,i}$ = 120; $K_{\omega,i}$ = 0.002}. This might not be the optimal design, but one of the suitable selections. Besides that, as described in Fig. 8(b), the motor torques are reduced suitably as the vehicle enter the slippery surface at 3.5 second. Consequently, the wheel velocities are always closed to the vehicle velocity, as shown in Fig. 8(a).

5.3 Test 2: Strategy 2 under the condition that an actuator is suddenly disconnected from the power source

Next, we will verify the hierarchically decentralized control system in Fig. 6. Unlike **Test 1**, the signal $\mathbf{T}_r$ is not distributed from the driver's driving command but from the signal T_g generated by the upper-layer controller C_g. The lower-layer is designed similarly to that in **Test 1**. There exist various options of the upper-layer controller C_g that satisfying the statement of **Proposition 6**. In this simulation, we consider a possible candidate of C_g as follows

$$C_g(s) = \frac{\eta_g}{s + \alpha_g} \tag{17}$$

By trial-and-error, a suitable pair of the global control gains is selected as { η_g = 100,000 ; α_g = 30 }. The vehicle is required to travel autonomously for 40 seconds on a hill with two corners, and the friction coefficient is μ = 0.45. Similarly to **Test 1**, we apply the optimal torque distribution law proposed by Fujimoto *et al* again to update the distribution ratio **k** at every control period. To challenge the proposed system, we assume that the 3rd wheel lost the electric power

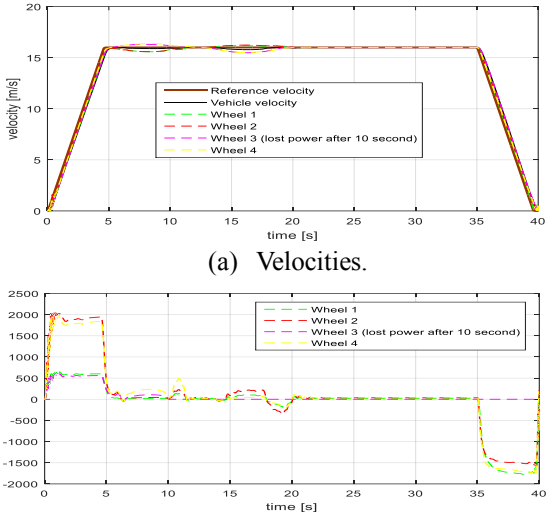

(a) Velocities.

(b) Motor torques.

Fig. 9. **Test 2**: Verification of Strategy 2.

(i.e., the electric wire is broken, or the wireless power transfer circuit is failure due to some reasons) at t_f = 10 second. We assume that this failure is diagnosed by the control system after Δt = 0.1 second. Since $t_f + \Delta t$, the upper-layer neglects the velocity measurement of the 3rd wheel; and it just aggregates the velocity measurement of the wheels numbered 1, 2, and 4. On the other hand, the global control signal is distributed to the wheels numbered 1, 2, and 4.

The simulation results of **Test 2** are drawn in Fig. 9. As seen in Fig. 9(b), the motor torques are distributed to follow the desired velocity pattern and minimize the motor output energy. Right after t_f, the motor torque of the 3rd wheel (the pink-dash-line) is always zero. It should be emphasized that the stability of both global and local motions of the vehicle is maintained even for this kind of a big failure. As shown in Fig. 9(a), the longitudinal velocities of all wheels, and the longitudinal velocity of the car body can successfully follow their reference pattern. The velocity tracking errors slightly increase during the cornering due to the influence of the lateral motion to the longitudinal motion.

6. CONCLUSIONS

The contribution of this paper is twofold. Firstly, we proposed a hierarchically decentralized model to capture the nonlinear dynamics of IWM-EV. This is a useful model for designing the IWM-EV motion control with proper treatment of physical interaction. Secondly, this paper introduces two new strategies for traction control of IWM-EV based on the glocal (global/local) concept with passivity theory. We have confirmed that the traction control system using either strategy can achieve both local objective (anti-slip) and global objective (system stabilization). Additional global objective can be achieved, such as optimal energy consumption. Moreover, the control systems can tolerate the actuator failures which might happen in realistic world.

To the best of our knowledge, this research is one of the first theoretical efforts towards the stability of the overall traction system, because the PBC systems can be designed in a very simple way. The complicated calculations such as linearization around operating point, pole-placement, and time-varying LQR are not necessary in our framework.

In future, we will implement the proposed control system for real-time experiments. Besides that, we will compare the performances of our strategy with other traction control strategies in the literature. How to apply passivity to full vehicle model with respect to longitudinal, lateral, and roll dynamics is certainly a challenge and interesting issue.

ACKNOWLEDGEMENTS

This work was supported in part by the Ministry of Education, Culture, Sports, Science and Technology in Japan through Grant-in-Aid for Scientific Research (B) No. 19H02377.

REFERENCES

Amada, J. and Fujimoto, H. (2012). "Torque Based Direct Driving Force Control Method with Driving Stiffness Estimation for Electric Vehicle with In-wheel-motor," *Proc. of the 38th Annual Conf. on IEEE IES*, pp. 4904-4909.

Amodeo, M., Ferrara, A., Terzaghi, R., and Vecchio, C (2010). "Wheel Slip Control via Second-Order Sliding-Model Generation," *IEEE Transactions on Intelligent Transportation Systems*, Vol. 11, Iss. 1, pp. 122-131.

Fujimoto, H., Saito, T., and Noguchi, T. (2004). "Motion Stabilization Control of Electric Vehicle Under Snowy Conditions Based on Yaw-Moment Observer," *Proc. of the IEEE Int. Workshop on Advanced Motion Control*, pp. 35-40.

Fujimoto, H and Harada, S (2015). "Model-Based Range Extension Control System for Electric Vehicles With Front and Rear Driving-Braking Force Distributions," *IEEE Transactions on Industrial Electronics*, Vol. 62, No. 5, pp. 3245-3254.

Hara, S., Imura, J., Tsumura, K., Ishizaki, T., and Sadamoto, T. (2015). "Glocal (Global/Local) Control Synthesis for Hierarchical Network System, *Proceedings of 2015 IEEE Conference on Control Applications*, pp.107-112.

Hatanaka, T., Chopra, N., Fujita, M., and Spong, M. W. (2015). "Passivity-Based Control and Estimation in Networked Robotics," *Communications and Control Engineering Series*, Springer-Verlag.

Hori, Y., Toyoda, Y., and Tsuruoka, Y. (1998). "Traction Control of Electric Vehicle: Basic Experimental Results Using the Test EV 'UOT Electric March'", *IEEE Transactions on Industry Applications*, Vol. 34, No. 5, pp. 1131-1138.

Hori, Y (2004). "Future Vehicle Driven by Electricity and Control-Research on 4 Wheel Motored UOT Mach II," *IEEE Trans. on Industrial Electronics*, Vol. 51, No. 5, pp. 954-962.

Jazar, Reza N. (2008). "Vehicle Dynamics: Theory and Applications," Springer, ISBN of 978-0-387-74243-4.

Khalil, H. K. (2002). "Nonlinear Systems," Prentice Hall.

Li, L., Kodama, S., and Hori, Y. (2006) "Design of Anti-Slip Controller for an Electric Vehicle with an Adhesion Status Analyzer Based on the EV Simulator," *Asian Journal of Control*, Vol. 8, No. 3, pp. 261-267.

Maeda, K., Fujimoto, H., and Hori, Y. (2013). "Four-wheel Driving-force Distribution Method for Instantaneous or Split Slippery Roads for Electric Vehicle," *Automatika*, Vol. 54, No. 1, pp. 103-113.

Nguyen, B-M., Wang, Y., Fujimoto, H., and Hori, Y. (2013) "Lateral Stability Control of Electric Vehicle Based on Disturbance Accommodating Kalman Filter Using the Integration of Single Antenna GPS Receiver and Yaw Rate Sensor," *Journal of Electrical Engineering & Technology*, vol. 8, no. 4, pp. 899-910.

Nguyen, B-M., Fujimoto, H., and Hara, S. (2016a). "Glocal Motion Control System of In-wheel-motor Electric Vehicles Based on Driving Force Distribution," *Proceedings of the SICE International Symposium on Control Systems*, pp. 15-22.

Nguyen, B-M., Hara, S., and Fujimoto, H. (2016b). "Stability Analysis of Tire Force Distribution for Multi-Actuator Electric Vehicles using Generalized Frequency Variable," *Proceedings of 2016 IEEE Conference on Control Applications*, pp. 91-96.

Nguyen, B-M., Hara, H., and Tsumura, K. (2017). "Hierarchically Decentralized Control for In-wheel-motored Electric Vehicles with Global and Local Objectives," *Proceedings of the 11th Asian Control Conference*, pp. 1176-1181.

Nguyen, B-M., Hara, S., Fujimoto, H., and Hori, Y. (2019a) "Slip Control for IWM Vehicles Based on Hierarchical LQR," *Control Engineering Practice*, Vol. 93, 104179.

Nguyen, B-M., Tsumura, K., and Hara, S. (2019b). "Interconnected Hierarchical Modelling and Passivity Based Motion Control of IWM Electric Vehicles," *Proceedings of IEEE Vehicle Power and Propulsion Conference*.

Ortega, R. and Spong, M. W. (1989). "Adaptive Control of Robot Manipulators: A Tutorial," *Automatica*, Vol. 25, No. 6, pp. 877-888.

Pacejka, H. B. (2012). "Tyre and Vehicle Dynamics," Third Edition, *Published by SAE International and Butterworth Heinemann* with a Product Code of R-418, ISBN of 978-0-0809-7016-5.

Sato, M., Yamamoto, G., Gunji, D., Imura, T., and Fujimoto, H. (2016). "Development of Wireless In-Wheel Motor Using Magnetic Resonance Coupling," *IEEE Transactions on Power Electronics*, Vol. 31, No. 7, pp. 5270-5278.

Shimizu, H. (2001) "Multi-purpose Electric Vehicle 'KAZ'," *IATSS Research*, Vol. 25, No. 2, pp. 96-97.

Suzuki, T. and Fujimoto, H. (2010). "Slip Ratio Estimation and Regenerative Brake Control without Detection of Vehicle Velocity and Acceleration for Electric Vehicle at Urgent Brake-turning," *Proceedings of the 11th IEEE International Workshop on Advanced Motion Control*, pp. 273-278.

Tsumura, K., Baros, S., Okano, K., and Annaswamy, A. M. (2018). "Design and Stability of Optimal Frequency Control in Power Networks: A Passivity-based Approach," *Proc. of 2018 ECC.*

Yin, D., Oh, S., and Hori, Y. (2009). "A Novel Traction Control for EV Based on Maximum Transmissible Torque Estimation," *IEEE Trans. on Industrial Electronics*, Vol. 56, No. 6, pp. 2086-2094.